Electronic Supporting Information

Dynamics of Intramolecular Spin Exchange Interaction of a Nitronyl Nitroxide Diradical in Solution and on Surface. Electrochemical and Magnetic Properties of Spin Labelled AuNPs and Au(111) Support.

V. Lloveras,[a] E. Badetti,[a] J. Veciana [a] and J. Vidal-Gancedo[a,*]

a. Institut de Ciència de Materials de Barcelona ICMAB (CSIC) and CIBER-BBN. Campus UAB, 08193 Bellaterra, Barcelona (Spain) and CIBER de Bioingeniería, Biomateriales y Nanomedicina (CIBER-BBN), Barcelona, Spain.

E-mail: j.vidal@icmab.es.

Contents

1. Experimental Section

1.1 Methods and chemicals

Solvents and starting materials were purchased from Aldrich. The control of the reaction and of the column chromatography was done with aluminium sheet covered with silica 60 F_{254} Merck. Silica column chromatography was carried out using silica gel 60 (35-70 mesh). Spin-labelled Au nanoparticles were purified by gel permeation chromatography using Bio-Beads SX-1 (Bio-Rad) gel and dichloromethane or toluene as eluent. Gold substrates were purchased from Arrandee (200–300 nm of gold on 1–4 nm of chromium on glass). Melting points were determined on a Kofler hot-plate melting point apparatus and are uncorrected. Elemental analyses for C, H and N are the average of two determinations. Matrix-assisted laser desorption ionization time-of-flight (MALDITOF) spectra were recorded on a BIFLEX spectrometer (Bruker-Franzen Analytik) equipped with a pulsed nitrogen laser (337 nm), operating in positive-ion reflector mode, using 19 kV acceleration voltage. IR spectra were recorded in the attenuated total reflectance mode (ATR) in a Perkin Elmer Spectrum One Fourier transform spectrometer. UV-Vis measurements were performed using a UV-Vis-NIR Cary 5000 spectrophotometer. The EPR spectra were recorded in a Bruker ELEXYS E500 X-band spectrometer equipped with a TE102 microwave cavity, a Bruker variable temperature unit, a field-frequency (F/F) lock system Bruker ER 033 M; line positions were determined with an NMR Gaussmeter Bruker ER 035 M. The modulation amplitude was kept well below the line width, and the microwave power was well below saturation. The cyclic voltammetric measurements were performed on a QUICELTRON potentiostat/galvanostat controlled by a personal computer and driven by dedicated software. Cyclic voltammetry was performed with a conventional three-electrode configuration consisting of platinum working and auxiliary electrodes and an Ag(s) reference electrode. HR-TEM analysis was performed in the "Servei de Microscòpia" of the Universitat Autònoma de Barcelona using a JEOL JEM-2010 model at 200 kV. Contact angle measurements were performed using an OCA 15 equipment supported with the software SCA20 (Dataphysics, Germany).

1.2 Sythesis of diradical 2

3,3′-Dithiodipropionic acid (57 mg, 0.27 mmol) was dissolved in dry THF (1 ml). At a temperature between 0-5ºC a solution of dicyclohexylcarbodiimide (DCC) (0.12 g, 0.60

mmol) in dry DCM (3 ml) was added to the dithiodipropionic acid and the solution were stirred during 5 minutes. Always at 0-5ºC 10 mg of 4-dimethylaminopyridine and a solution of 2-(4-hydroxy-phenyl)-α-nytronyl nitroxide radical (0.15 g, 0.60 mmol) in 3 ml of dry DCM were added to the reaction mixture and the solution was stirred under argon for 14 h at r.t. The reaction mixture was filtered, and excess of 2-(4-hydroxy-phenyl)-α-nytronyl nitroxide radical was removed by extraction with distilled water (2 × 5 ml). The crude product was purified by flash chromatography using 3:2 AcOEt : $CHCl_3$ mixture (R_f = 2.33). Yield: 0.12 g (66%), mp 163-165 °C (dec.). Anal. calcd for $C_{32}H_{40}N_4O_8S_2$, %: C 57.18, H 6.00, N 8.33; found %: C 57.07, 57.11; H 5.97, 5.96; N 8.15, 8.25. MALDI-TOF, *m*/*z*: 672.3 [M]. IR (ATR) ν: 2989, 2923, 2852, 1753, 1603, 1422, 1392, 1361, 1301, 1207, 1165, 1113, 1014 cm^{-1}. UV-Vis (CH_2Cl_2) λ_{MAX}: 228, 350, 366, 600 nm.

1.3. Preparation of spin-labelled Au nanoparticles

Au nanoparticles protected by tri-*n*-octylamine (*ca.* 3.5 nm) were synthesized using published procedures.[1] For the ligand exchange reaction, the concentration of nanoparticles was calculated assuming molecular formula $Au_{300}R_{100}$ were R is the alkanethiol ligand.

1.3.1. Sythesis of AuNPs 3

0.035 g (0.10 mmol) of a 1% aqueous hydrogen tetrachloroaurate trihydrate solution was dried first evaporating in a rotary evaporator at 60ºC and then in the vacuum line at 60ºC for 2 h to remove the water, then 45 ml toluene and 4 g (0.11 mmol) of tri-*n*-octylamine were added. The mixture was sonicated for 20 min until a clear yellow solution was obtained, indicating that $HAuCl_4$ was fully dissolved in toluene. 0.5 mL aqueous solution containing 0.02 g (0.53 mmol) of $NaBH_4$ was then added under vigorous magnetic stirring to reduce $HAuCl_4$. The colour of the solution quickly turned from yellow to red. After 2 h (with the flask opened to air) half of the flask volume was removed under vacuum and a dichloromethane solution (3 mL) of diradical **2** (0.03 g, 0.05 mmol) was added and the reaction left to proceed for 17 h (with the flask closed to air with a septum). The excess of solvent was removed until 3 or 4 mL under vacuum and 20 mL methanol were then added and centrifugated. The methanol phase was red wine and it contained the nanoparticles. The methanol was removed under vacuum to give a violet solid. The solid was redissolved in the minimum amount of

dichloromethane and purified by gel permeation chromatography using Bio-Beads SX-1 (Bio-Rad) as a stationary phase and dichloromethane as eluent. The purified sample was evaporated under a stream of nitrogen, dissolved in DCM and analysed by EPR.

1.3.2. Sythesis of AuNPs 4

1.3.2.1. Sythesis of AuNPs stabilized by tri-*n*-octylamine in toluene

0.035 g (0.10 mmol) of a 1% aqueous hydrogen tetrachloroaurate trihydrate solution was dried first evaporating in a rotary evaporator at 60ºC and then in the vacuum line at 60ºC for 2 h to remove the water, then 45 ml toluene and 4 g (0.11 mmol) of tri-*n*-octylamine were added. The mixture was sonicated for 20 min until a clear yellow solution was obtained, indicating that $HAuCl_4$ was fully dissolved in toluene. 0.5 ml aqueous solution containing 0.02 g (0.53 mmol) $NaBH_4$ was then added under vigorous magnetic stirring to reduce $HAuCl_4$. The colour of the solution quickly turned from yellow to red. After 2 h (with the flask opened to air) half of the flask volume was removed under vacuum and 15 ml methanol (x2) were then added and centrifugated. The toluene phase, separated from the methanol, was red wine and it contained the nanoparticles stabilized by tri-*n*-octylamine.

1.3.2.2. Ligand exchange reaction

At this toluene phase containing the stabilized gold nanoparticles were added 0.03 g (0.05 mmol) of diradical **2** dissolved in 3 ml of DCM and the mixture were stirred overnight at room temperature. The excess of solvent was removed under vacuum and 15 ml methanol were then added and centrifugated to eliminate crashed nanoparticles. The methanol phase was red wine and it contained the nanoparticles. The methanol was removed under vacuum to give a violet solid. The solid was redissolved in the minimum amount of dichloromethane and purified by gel permeation chromatography using Bio-Beads SX-1 (Bio-Rad) as a stationary phase and dichloromethane as eluent. The purified sample was evaporated under a stream of nitrogen, dissolved in DCM and analysed by EPR.

1.3.3. Sythesis of AuNPs 5

A toluene phase containing gold nanoparticles stabilized by tri-*n*-octylamine was obtained as described in **paragraph 1.3.2.1**. At this toluene phase were added 0.03 g (0.05 mmol) of diradical **2** dissolved in 3 ml of DCM and the mixture were stirred during 1 night at room temperature and then, at 32ºC for 1 h. The excess of solvent was

removed under vacuum and 15 ml methanol were then added and centrifugated to eliminate crashed nanoparticles. The methanol phase was red wine and it contained the nanoparticles. The methanol was removed under vacuum to give a violet solid. The solid was redissolved in the minimum amount of dichloromethane and purified by gel permeation chromatography using Bio-Beads SX-1 (Bio-Rad) as a stationary phase and dichloromethane as eluent. The purified sample was evaporated under a stream of nitrogen, dissolved in DCM and analysed by EPR. HR-TEM: 3.24 ± 0.35 nm. IR (ATR) ν: 2954, 2925, 2855, 1747, 1609, 1508, 1466, 1364, 1203, 1167, 1118, 1021 cm^{-1}. UV-Vis (CH_2Cl_2) λ_{MAX}: 301, 540 nm.

1.3.4. Sythesis of AuNPs 6

A toluene phase containing gold nanoparticles stabilized by tri-*n*-octylamine was obtained as described in **paragraph 1.3.2.1**. At this solution, 0.030 g (0.05 mmol) of diradical **2** dissolved in 3 ml of DCM were added and the mixture was stirred overnight at 35ºC. The excess of solvent was removed under vacuum and 15 ml methanol were then added and centrifugated to eliminate crashed nanoparticles. The methanol phase was red wine and it contained the nanoparticles. The methanol was removed under vacuum to give a violet solid. The solid was redissolved in the minimum amount of dichloromethane and purified by gel permeation chromatography using Bio-Beads SX-1 (Bio-Rad) as a stationary phase and dichloromethane as eluent. The purified sample was evaporated under a stream of nitrogen, dissolved in DCM and analysed by EPR. HR-TEM: 2.30 ± 0.99 nm. IR (ATR) ν: 2954, 2925, 2856, 1736, 1608, 1455, 1359, 1283, 1213, 1176, 1132, 840 cm^{-1}. UV-Vis (CH_2Cl_2) λ_{MAX}: 364, 530 nm.

1.3.5. Sythesis of AuNPs 7

A toluene phase containing gold nanoparticles stabilized by tri-*n*-octylamine was obtained as described in **paragraph 1.3.2.1**. At this solution, 0.016 g (0.02 mmol) of diradical **2** dissolved in 1 ml of DCM/toluene anhydrous (1/1) were added. The mixture was stirred during 4h and 30 min at 40 ºC under inert atmosphere, and uniformly stirring the solution using paddles. The excess of solvent was removed under vacuum and the solid obtained was redissolved in the minimum amount of dichloromethane and purified by gel permeation chromatography using Bio-Beads SX-1 (Bio-Rad) as a stationary phase and dichloromethane as eluent. The purified sample was evaporated

under a stream of nitrogen, dissolved in DCM and analysed by EPR. HR-TEM: 2.06 ± 0.27 nm. IR (ATR) ν: 3025, 2962, 2925, 2340, 1740, 1602, 1452, 1362, 1258, 1210, 1084, 1013, 867 cm^{-1}. UV-Vis (CH_2Cl_2) λ_{MAX}: 267, 366, 530 nm.

1.4. Preparation of SAMs on Au(111) with diradical 2

Au(111) was prepared by butane flame annealing in air after cleaning the substrate, with acetone, dichloromethane, ethanol, (5 min each in ultrasonic bath), and then in piranha solution (1:3 H_2O_2/H_2SO_4) for 4 min. After cleaning piranha, the substrates were vigorously rinsed with MQ water and dried under N_2 stream.[2] These substrates, freshly cleaned, were immersed in a 1 mM THFanh solution of diradical **5** under light exclusion during 3h at 40ºC and then during approximately 10h at room temperature, under argon atmosphere. After this time the monolayer were vigorously rinsed with abundant THF, to ensure that there were no physisorbed material on the substrate, and dried under N_2 stream. The resulting SAMs were characterized by contact angle (L: 73.8º, 78.1º, 83.8º; R: 72.1º, 77.6º, 79.9º), XPS, and ToF-SIMS (see text). The electrochemical and magnetic properties were investigated by cyclic voltammetry (CV) and EPR respectively (see text).

2. Experimental spectra of diradical 2.

UV-Vis

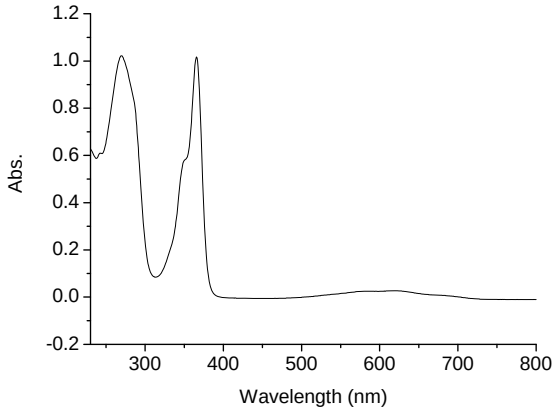

IR

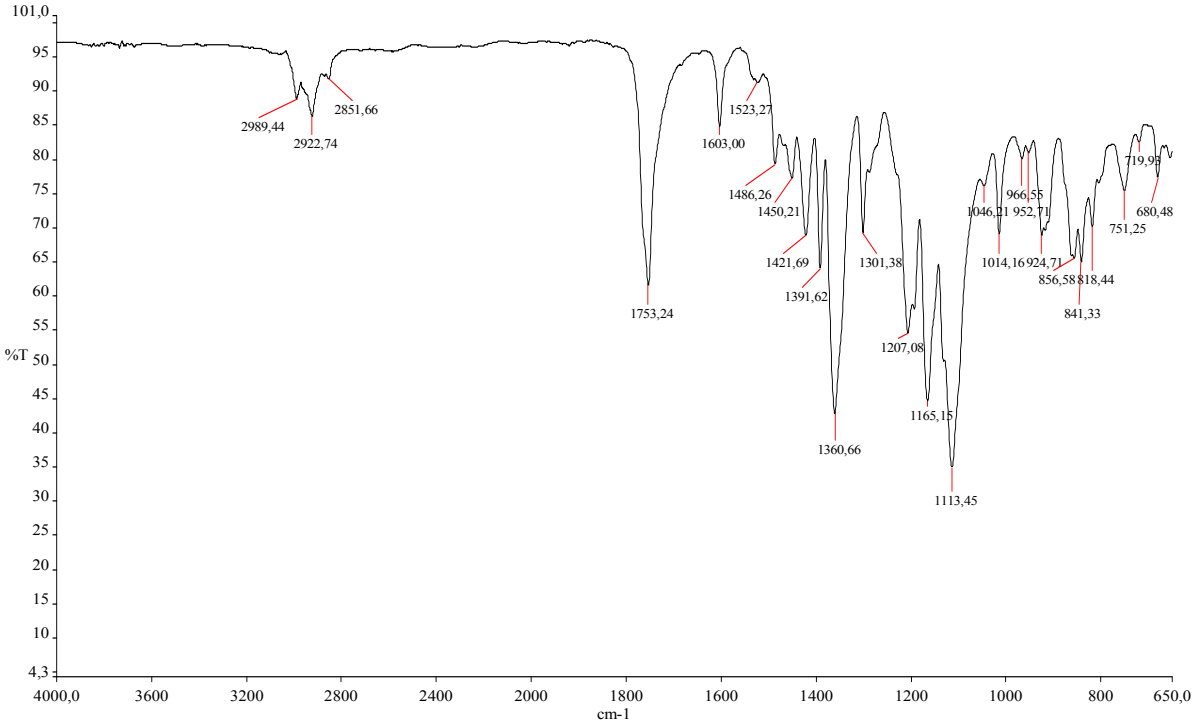
101,0
95
90
85
80
75
70
65
60
55
%T 50
45
40
35
30
25
20
15
10
4,3
4000,0
3600
3200
2800
2400
2000
1800
1600
1400
1200
1000
800
650,0
cm-1
2989,44
2922,74
2851,66
1753,24
1603,00
1523,27
1486,26
1450,21
1421,69
1391,62
1360,66
1301,38
1207,08
1165,15
1113,45
1046,21
1014,16
966,55
952,71
924,71
856,58
841,33
818,44
751,25
719,93
680,48

MALDI-TOF

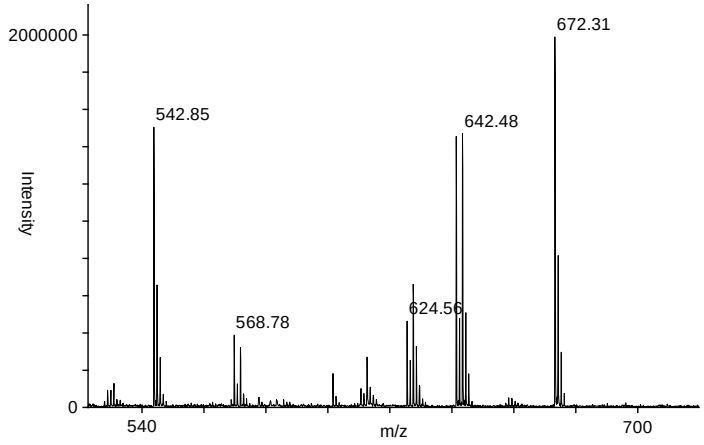
2000000
Intensity
0
540
m/z
700
542.85
568.78
624.56
642.48
672.31

3. EPR figures of radical derivative 1 and diradical 2.

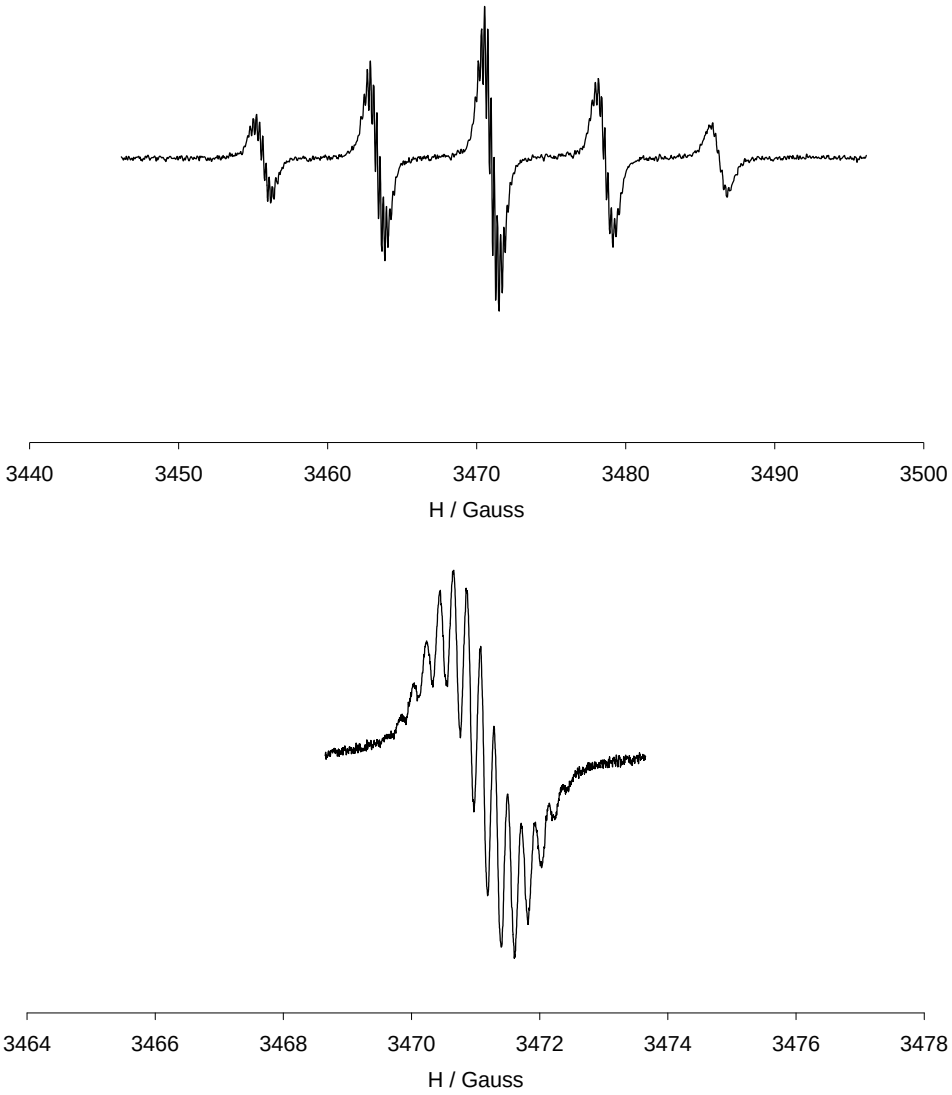

Fig. S1. Up) EPR spectrum of nitronyl nitroxide derivative **1**. Down) EPR spectrum of the first line of the nitronyl nitroxide derivative **1** spectrum.

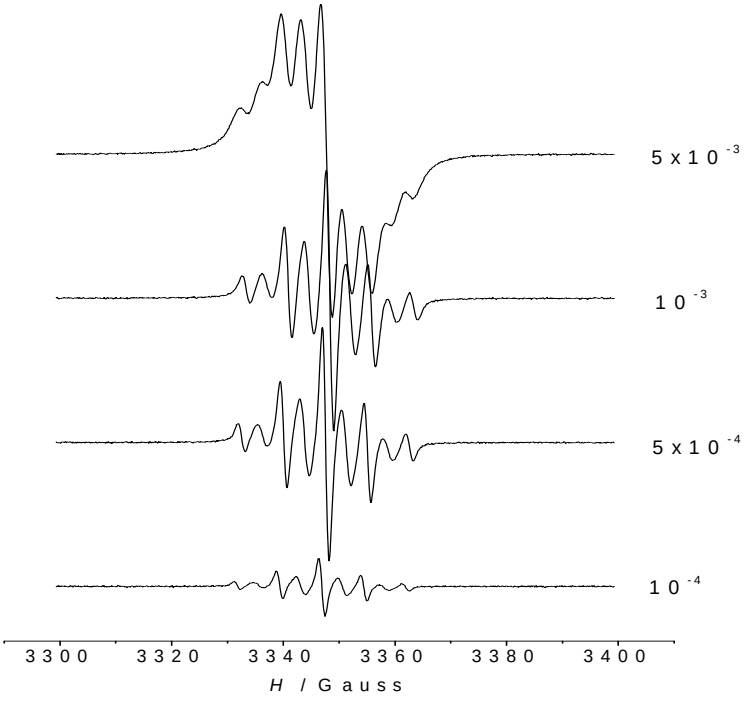

Fig. S2. EPR spectra of diradical **2** in dichloromethane:toluene 1:1 at different concentrations, from $5x10^{-3}$ to 10^{-4} M, at 300 K.

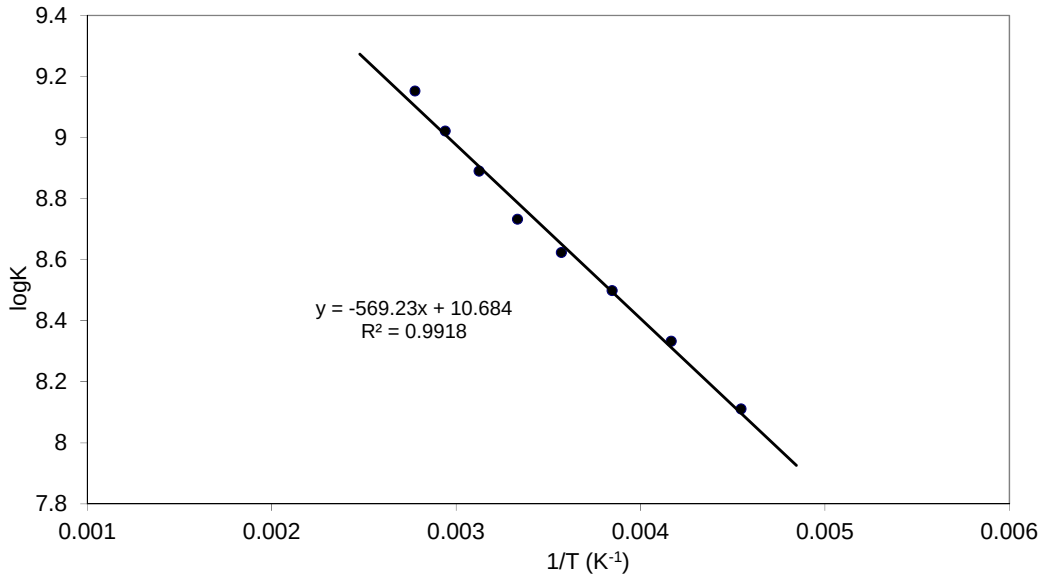

Fig. S3. Arrhenius plot of the rate constants over the 220–360 K temperature range for diradical **2**.

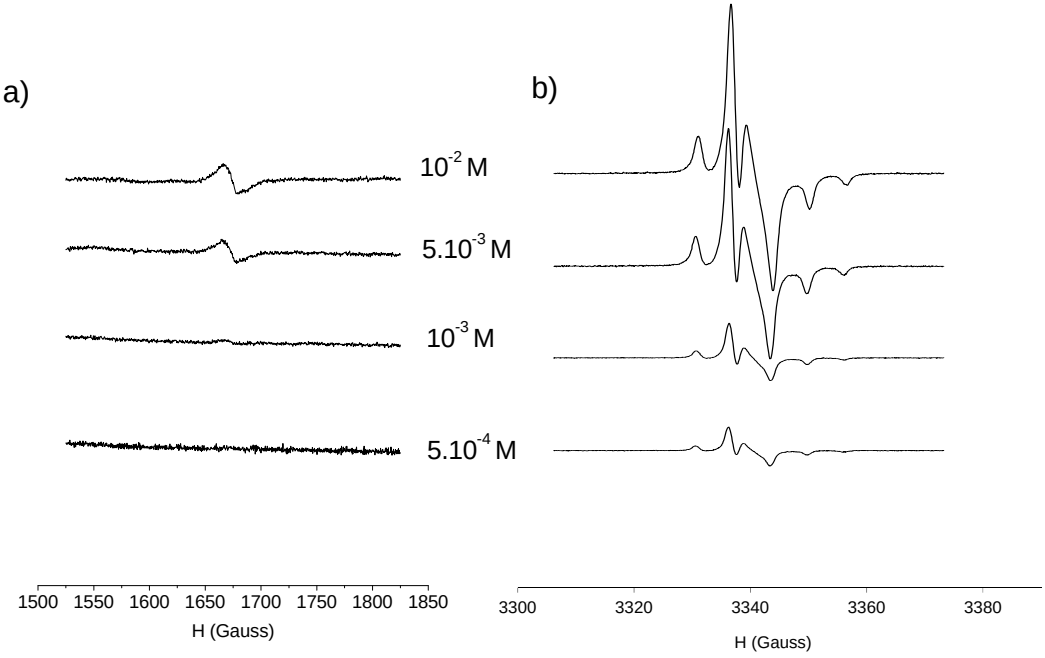

Fig. S4. EPR spectra of diradical **2** in frozen conditions (130 K) in dichloromethane:toluene 1:1 at different concentrations, from 10^{-2} to 10^{-4} M. a) The |Δms| = 2 transition at half field. b) EPR |Δms| = 1 signal.

4. Reaction Scheme and EPR charaterization of AuNPs 3.

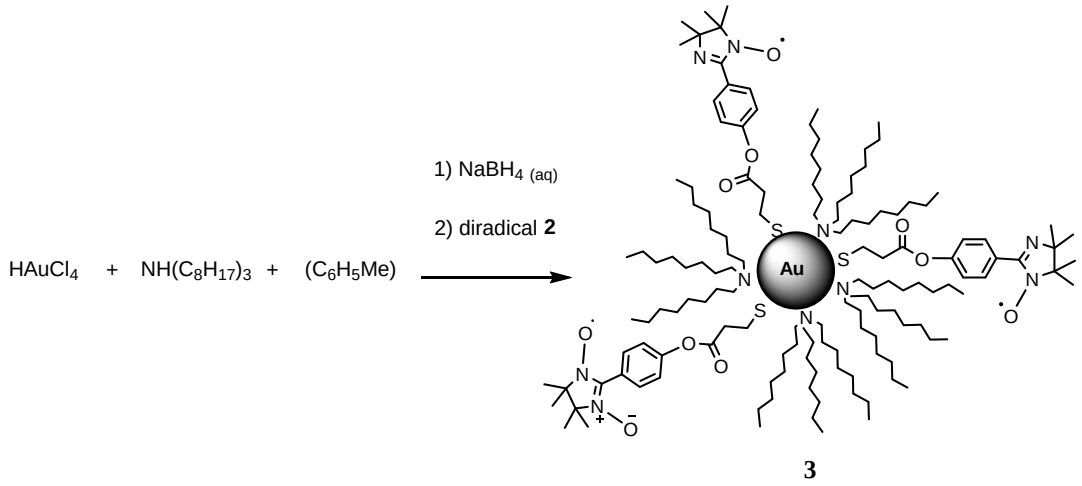

Scheme S1. Synthesis of AuNPs **3** containing nitronyl nitroxide and imino nitroxide radicals.

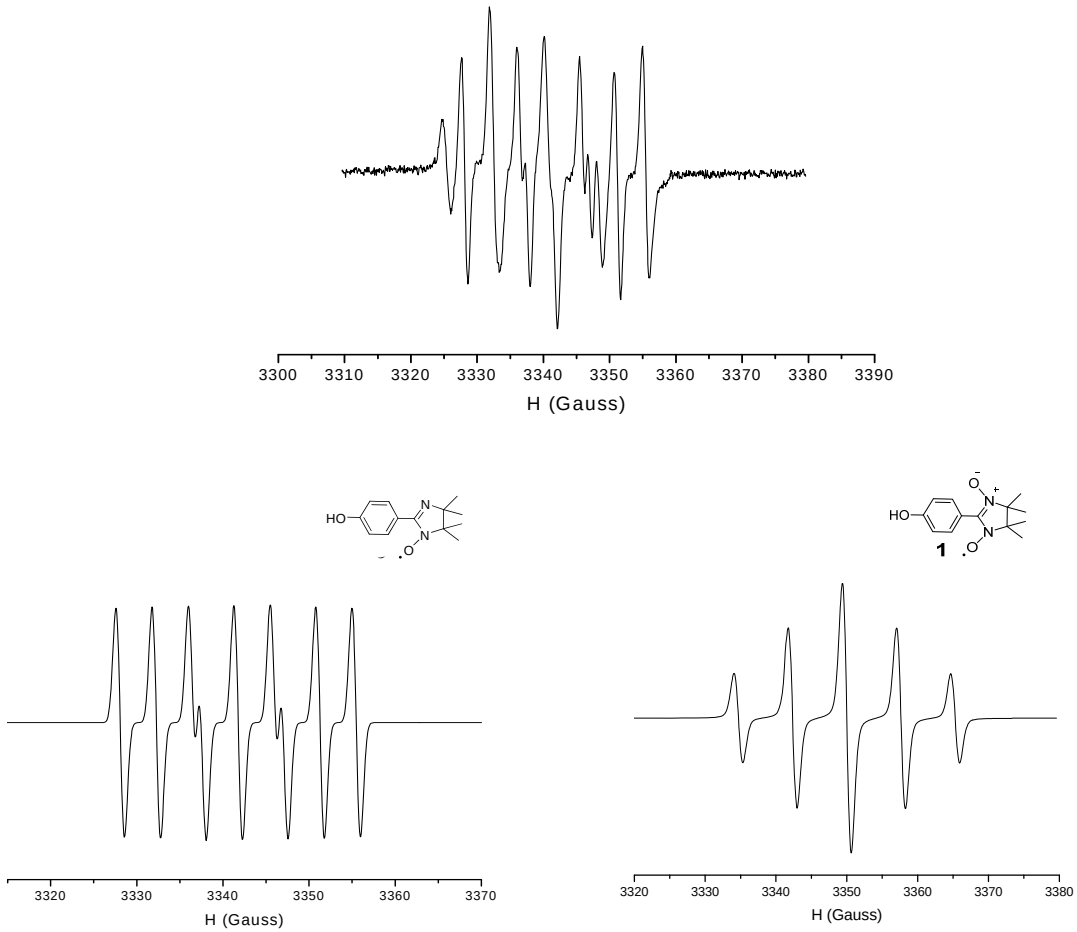

Fig. S5. Up) Experimental EPR spectrum of AuNPs **3** in CH_2Cl_2 at 300 K. Down) Simulated EPR spectrum of 4-hydroxyphenyl imino nitroxide (left) and 4-hydroxyphenil nitronyl nitroxide (right).

5. UV-Vis, IR and HR-TEM characterization of AuNPs 5.

We repeated the same reaction conditions than AuNPs **4** but stirring the mixture first overnight at room temperature and then at 32ºC for 1h (Scheme S2). In this case, the corresponding solution EPR spectrum of the purified nanoparticles (**5**, Fig. 4) also showed a five-line pattern but with very little contribution of a broad line, attributed to slightly higher coverage. The surface plasmon band observed by UV-Vis spectroscopy at 530 nm (Scheme S2, Fig. b) indicated that these nanoparticles had a diameter of *ca.* 3 nm.[3] HR-TEM microscopy confirmed the presence of homogeneous and well dispersed nanoparticles with a diameter of 3.24 ± 0.35 nm. The electron diffraction of these nanoparticles (Scheme S2) showed the characteristic pattern of face-centered cubic (fcc) Au(0) with the average *d*-spacing values 2.36; 2.04; 1.44; 1.23; 1.18 Å. The IR of AuNPs **5** can be shown in Fig. S6.

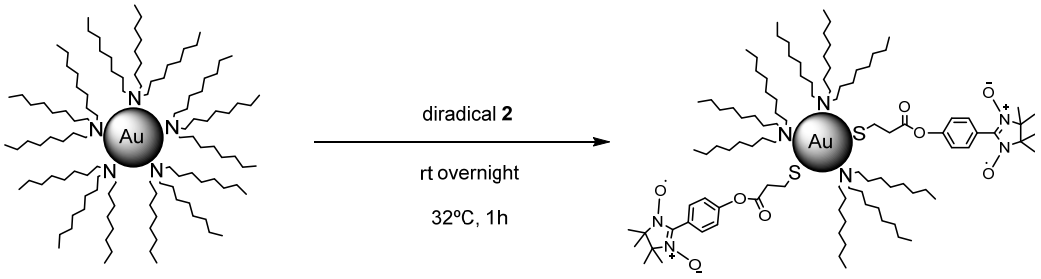

AuNPs **5**

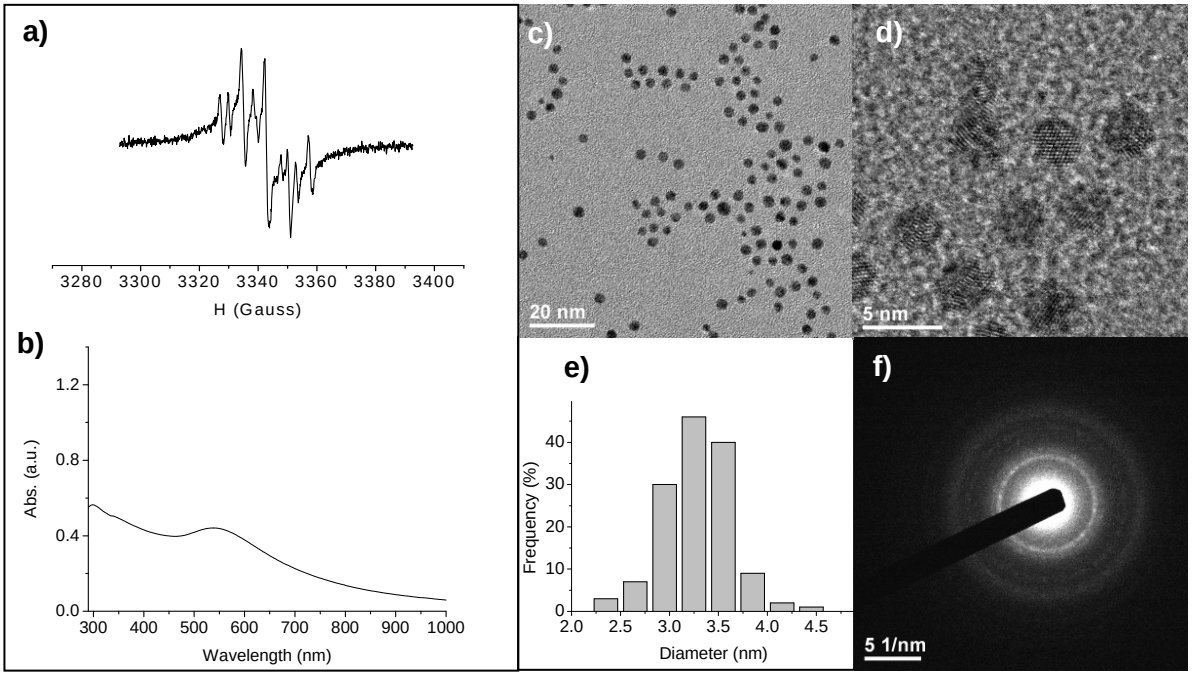

Scheme S2. Up) Synthesis of AuNPs **5**. Down) Characterization of nanoparticles AuNPs **5**: a) Solution EPR spectrum in dichloromethane at 300 K. b) UV-Vis spectrum. c) and d) HR-TEM pictures. e) Core size distribution histogram (average 3.24 ± 0.35 nm). f) Electron diffraction patterns corresponding to Au(0) fcc of AuNPs **5**.

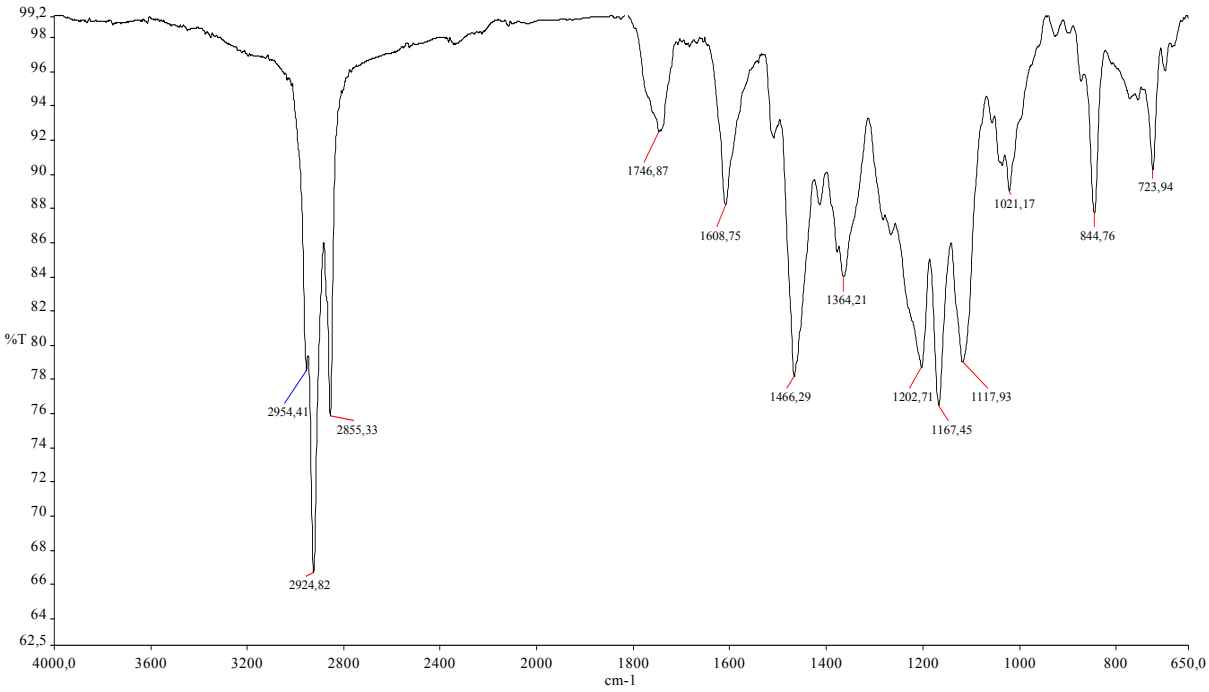

Fig. S6. IR spectrum of AuNPs **5.**

6. UV-Vis, IR, HR-TEM and TGA characterization of AuNPs 6.

As the temperature seemed to be an important parameter to increase the coverage, we let stirring the ligand exchange reaction overnight at 35 ºC (AuNPs **6**, Scheme S3). The solution EPR spectrum at 300 K (Fig. 4) indicated an increase in the coverage of these nanoparticles as there was more contribution of the enveloping single broad line. The surface plasmon band observed by UV-Vis spectroscopy at 530 nm (Scheme S3, Fig. b) indicated that these nanoparticles had less diameter than AuNPs **5**, which was confirmed by HR-TEM microscopy (Scheme S3). The Thermogravimetric Analysis (TGA) of these NPs showed that 17.99 % of the total mass of nanoparticles was organic coating (Fig. S7). From these data and TEM analysis we could estimate the maximum number of radicals per nanoparticle possible (48) and the packing density (see Table S1), which are in agreement with previous data reported in the literature.[4] As the particles formed in these conditions were less homogeneous than in the previous reaction (pictures and distribution histogram of Scheme S3), we uniformly stirred the

solution using mechanical stirring with paddles in the following reactions. The IR of AuNPs **6** can be shown in Fig. S8.

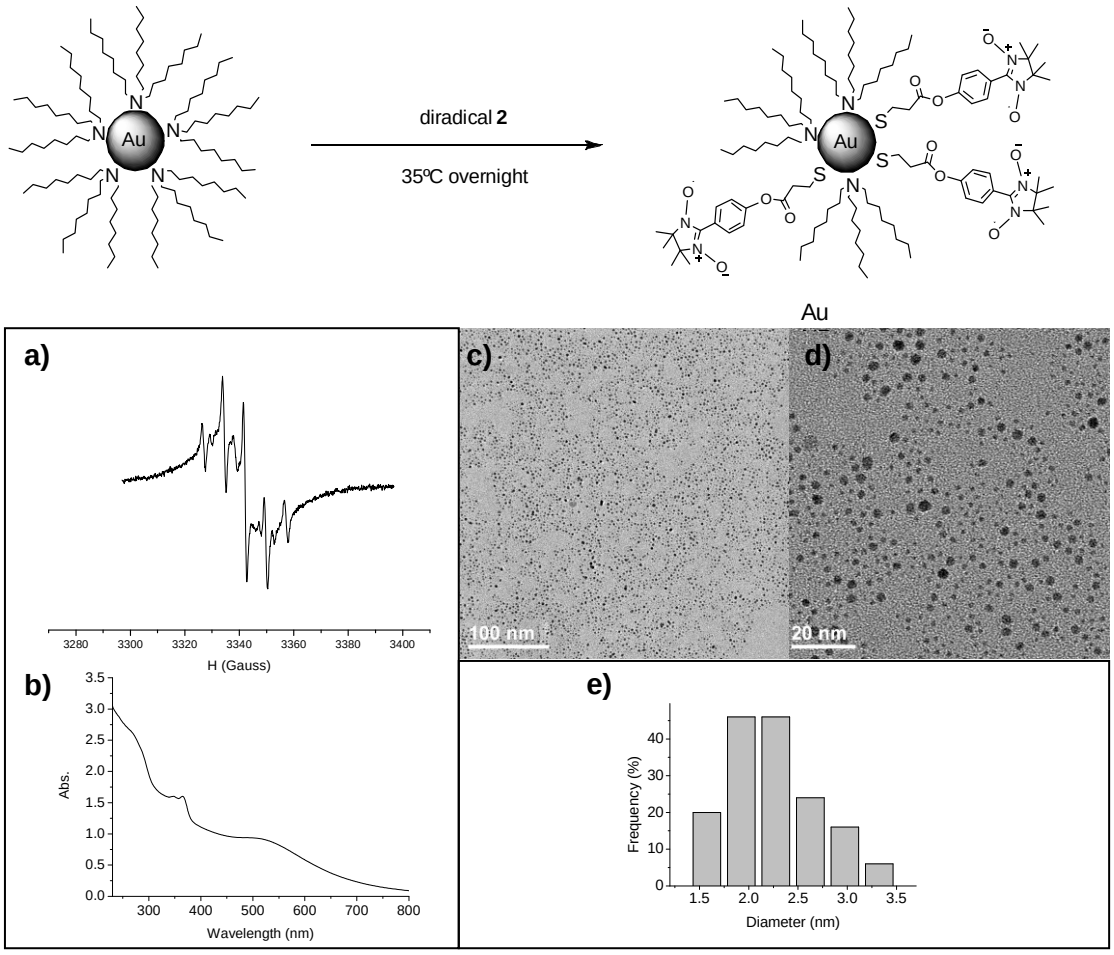

Scheme S3. Up) Synthesis of AuNPs **6**. Down) Characterization of nanoparticles AuNPs **6**: (a) Solution EPR spectrum in dichloromethane at 300 K. (b) UV-Vis spectrum. (c) and (d) HR-TEM pictures. (e) Core size distribution histograms (average 2.30 ± 0.99 nm).

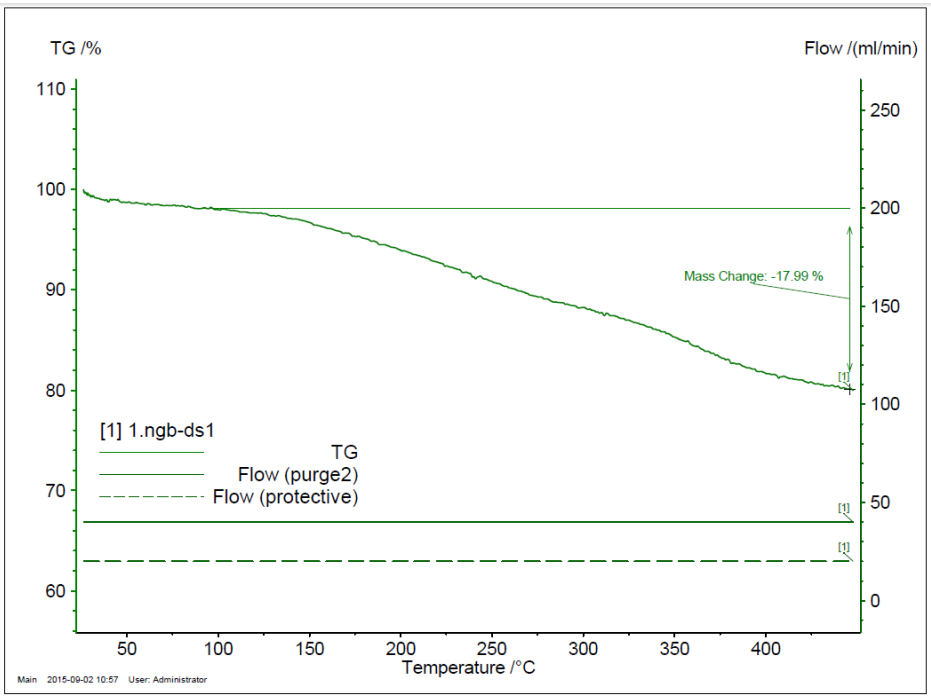

Fig. S7. TGA of AuNP **6**.

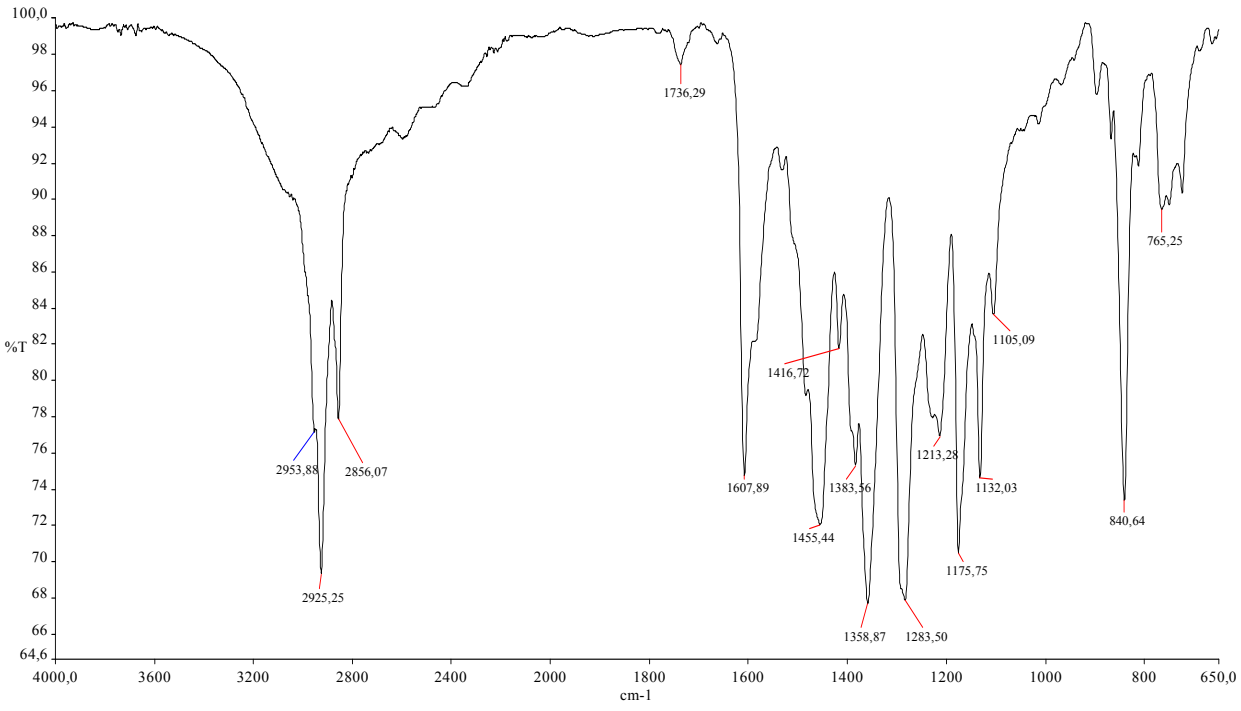

Fig. S8. IR of AuNP **6**.

7. TGA, EDX, and IR spectra of AuNPs 7.

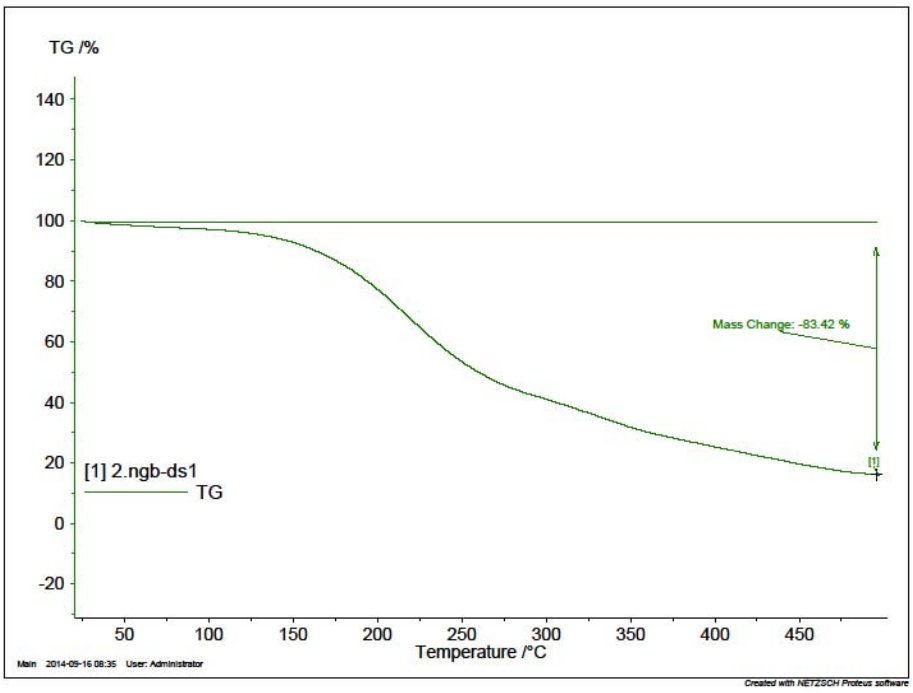

Fig. S9. TGA of AuNP **7**.

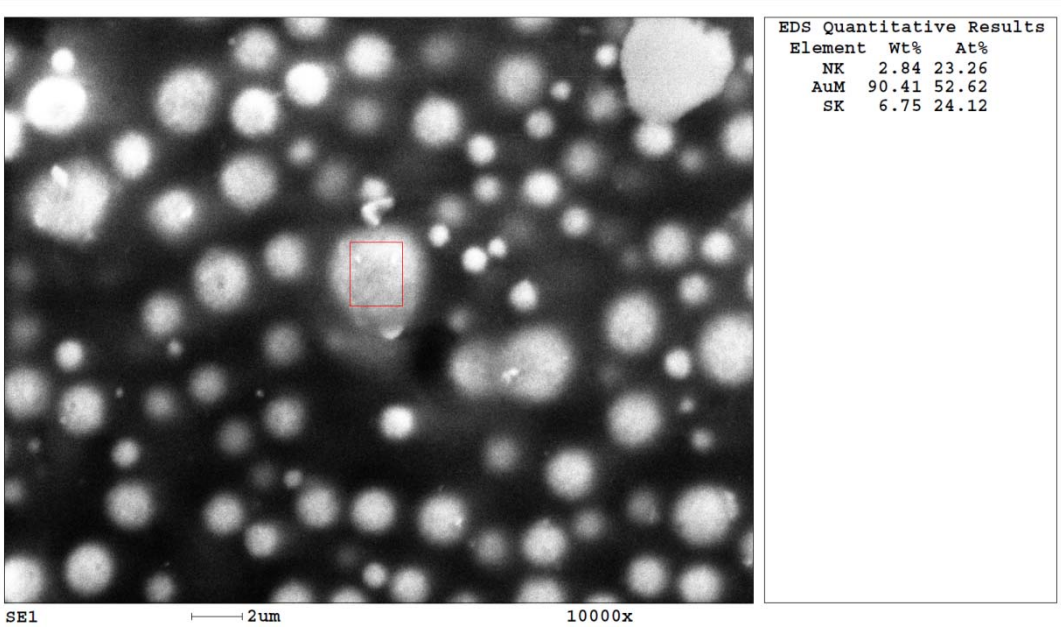

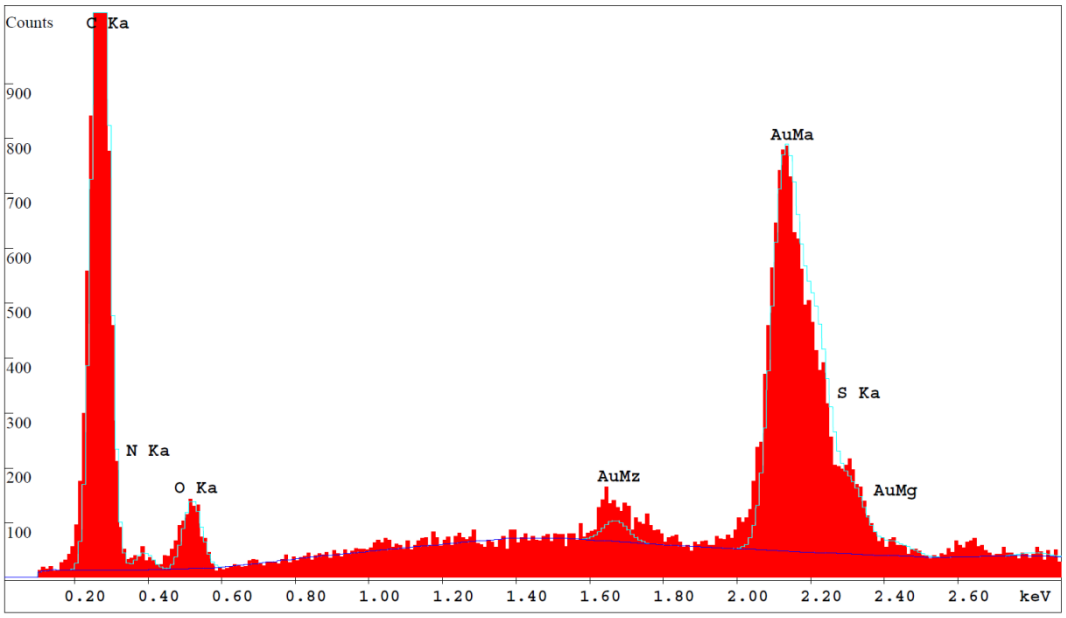

Fig. S10. EDX of AuNP **7**.

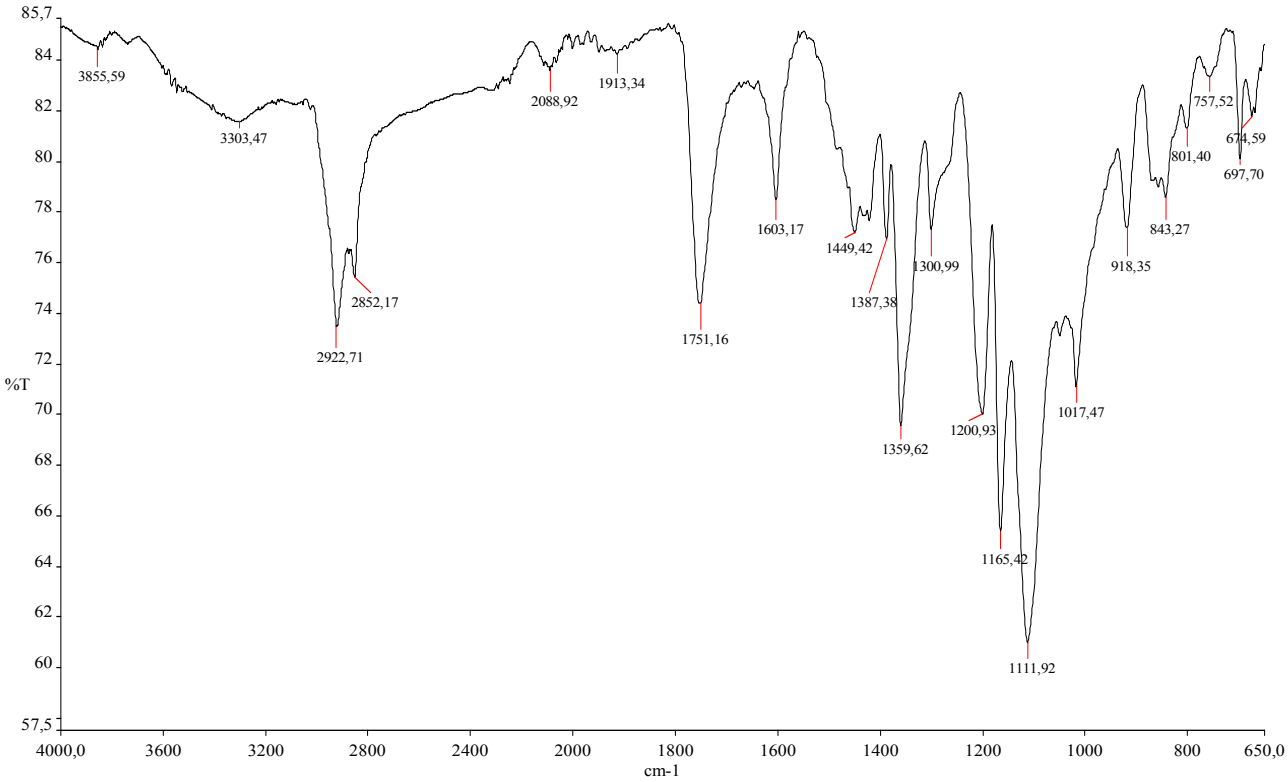

Fig. S11. IR spectrum of AuNPs **7**.

8. Calculus of the maximum number of radicals per NP and packing density.

Table S1. Calculus of the maximum number of radicals per NP and packing density of AuNPs **6** and **7**.

NP	**TEM**	**TGA**					
	Particle diameter (nm)	**% organics**	**% gold**	**Nº gold atoms per nanoparticle**	**Maximum nº of radicals per nanoparticle(1)**	**AuNP area ($Å^2$)**	**Maximum packing density S_0 ($Å^2$) (1)**
6	2.30	17.99	82.01	376	48	1661.9	34.6
7	2.06	83.42	16.58	271	795	1333.2	1.7

(1) As an approximation, we have assumed that all organic ligands are spin-labeled (using the molecular weight of the S-CH_2-CH_2-CO-O-ph-nitronyl nitroxide). Therefore, these data are the maximum number of radicals per particle possible and the maximum packing density possible.

Assuming the spherical shape of nanoparticles, the average number of gold atoms per AuNP was calculated according to Huo *et al.* (*Colloids Surf. B* **2007**, *58*, 3-7) equation:

$$N = \pi \rho D^3/6 M$$

N = number of atoms per nanoparticle
ρ = density for fcc gold = 19.3 g/cm^3
D = average diameter of nanoparticles, in nm
M = atomic mass of gold

Although the data are an approximation, there are higher number of radicals per NP and packing density in AuNPs **7** than in AuNPs **6**, which is in agreement with the EPR spectra shape obtained. Although not all the ligands are labelled and hence the value of the packing density will increase, the one for NP **7** (1.7 $Å^2$) seems to be very high: the usual packing density for the thiolate self-assembling of the gold nanoparticle surface reported by the community is between 15 and 20 $Å^2$ (see for example Kimura, Langmuir 1999, 15, 1075-1082 or Chechik Faraday Discussions 2004, 125, 279). However, we have reported recently very high number of radicals per NP and packing density in AuNPs densely coated with TEMPO radicals (515, 1527 and 2689 as

maximum number of radicals per NP and 6.2, 6.4 and 5.3 as maximum packing density, respectively).[1]

9. XPS and TOF-SIMS of the SAM on Au(111).

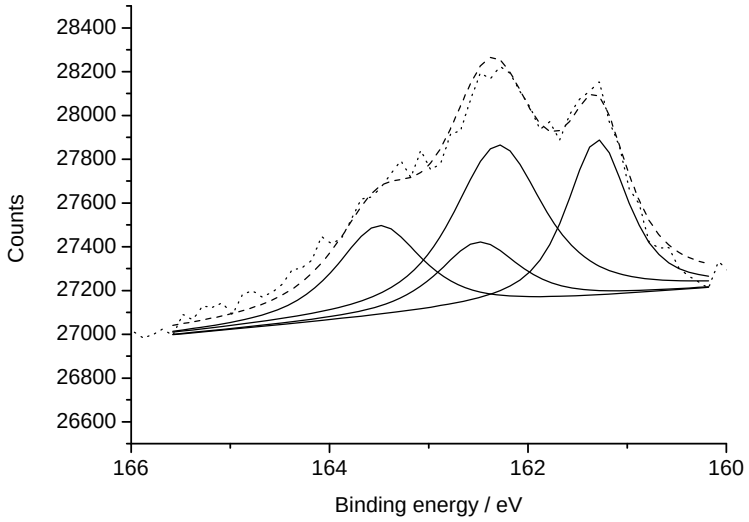

Fig. S12. XPS spectrum of S2p of the SAM. The experimental spectrum (dotted line) is deconvoluted in two doublets (solid lines) at 162.3 and 163.5 eV with an intensity ratio of 1.9 : 1 and at 161.3 and 162.5 eV with the same intensity ratio. The theoretical simulation (dashed line) fits very well with the experimental one.

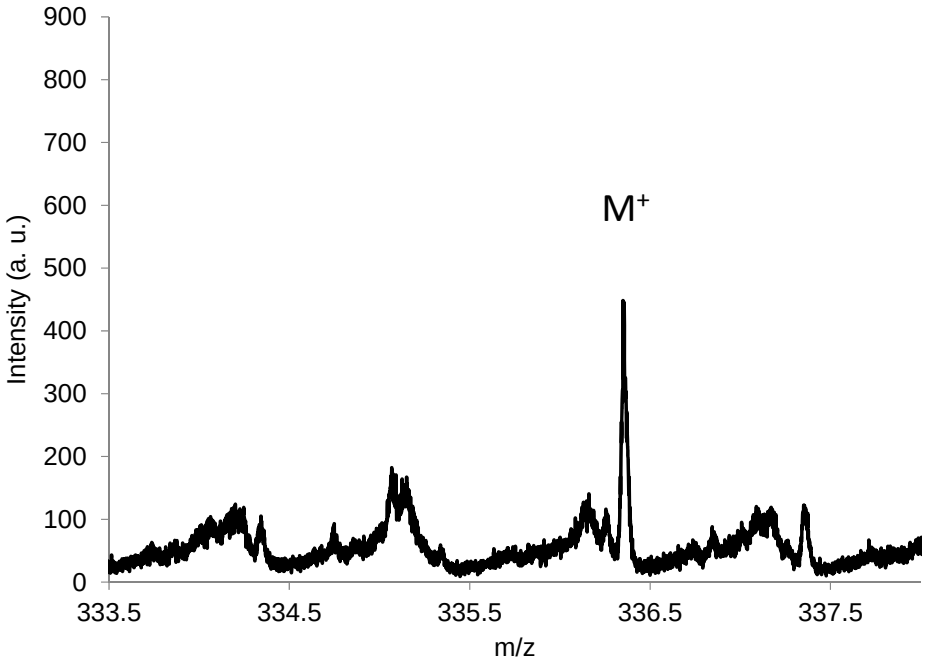

Fig. S13. TOF-SIMS spectrum of $SC_{12}H_{21}N_2O_2$ (M^+) of the SAM.

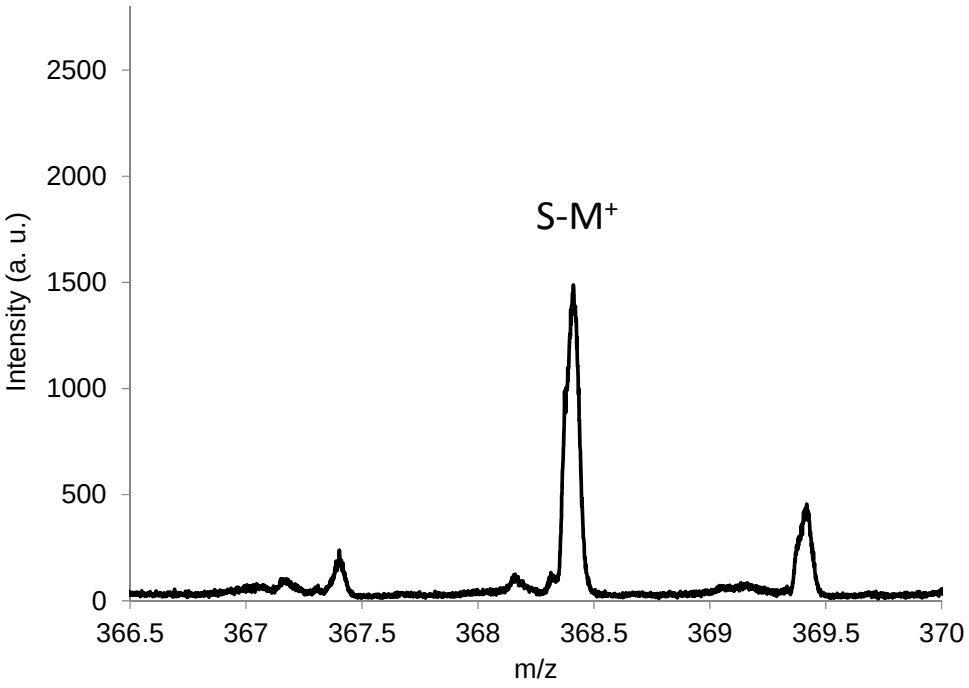

Fig. S14. TOF-SIMS spectrum of S-$SC_{12}H_{21}N_2O_2$ (S-M^+) of the SAM.

10. References

[1] V. Lloveras, E. Badetti, V. Chechik and J. Vidal-Gancedo, *J. Phys. Chem. C,* 2014, **118**, 21622.

[2] N. Crivillers, M. Mas-Torrent, J. Vidal-Gancedo, J. Veciana and C. Rovira, *J. Am. Chem. Soc.*, 2008, **130**, 5499.

[3] a) S. Link and M. A. El.Sayed, *J. Phys. Chem. B,* 1999, **103**, 4212; b) W. Haiss, N. T. K. Thanh, J. Aveyard and D. G. Fernig, *Anal. Chem*., 2007, **79**, 4215.

[4] V. Chechik, H. J. Wellsted, A. Korte, B. C. Gilbert, H. Caldararu, P. Ionita and A. Caragheorgheopol, *Faraday Discuss.*, 2004, **125**, 279.